Methods to Analyse the Texture of Alginate Aerogel Microspheres

*Romain Valentin, Karine Molvinger, Françoise Quignard, Francesco Di Renzo**

Laboratoire Matériaux Catalytiques et Catalyse en Chimie Organique, UMR 5618 ENSCM-CNRS-UM1, ENSCM, 8 Rue de l'Ecole Normale, 34296 Montpellier, France
Email: direnzo@cit.enscm.fr

Summary: Nitrogen adsorption at 77 K has been applied to the study of the texture of alginate aerogel microspheres obtained by CO_2 supercritical drying of alcogels. The limited volume shrinkage suggests that the aerogels preserve the texture of the hydrogels. Alginate aerogels presents a N_2 adsorption at small pressure higher than reference non-porous silica, to be attributed to the polarity of the surface or to a small microporous volume. The aggregated nanobead strings of the guluronic-rich gels accounts for a significant mesoporosity. The N_2 adsorption results correspond to electron microscopy observations for features smaller than 50 nm.

Keywords: aerogel; alginate; biopolymer; nitrogen adsorption; supercritical drying; textural characterisation

Introduction

Alginates are abundant polysaccharides produced by brown algae, mainly composed of (1-4) linked β-D-mannuronic (M) and α-L-guluronic (G) residues (figure 1), in varying proportions, sequence and molecular weight. The use of alginate in most applications lies in its ability to form heat-stable strong gels with divalent or trivalent cations, most generally Ca^{2+}. The strength of the gel has been attributed to the electrostatical interaction of the cation with the guluronic residues, affording a three-dimensional network described by an "egg-box" model.[1] Alginates are used as thickeners in the food industry as well as for the encapsulation of bioactive materials like drugs,[2] proteins,[3] living cells,[4] and enzymes.[5]

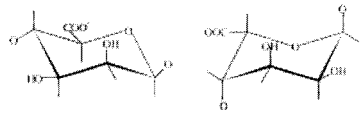

Figure 1. The alginate monomers: (left-hand) β-D-mannuronate (**M**) and (right-hand) α-L-guluronate (**G**).

 DOI: 10.1002/masy.200550410

The structure of alginate hydrogels has been widely studied by scanning electron microscopy. Structural features in the size range 1-100 μm have been observed[6, 7] and early attributed to modifications of the gel due to the drying process.[8] The presence of large cavities in the dried material has been confirmed by neutron diffusivity measurements[9] but it is still subject of debate at which point structural features like micrometric shafts or crevices are already present in the hydrogel.[9, 10] The presence of a smaller porosity with a size scale of tens of nanometers is evidenced by the easy accessibility of the alginate hydrogels, through which macromolecules up to 20,000 Da can freely diffuse.[11, 12] This porosity seems to be delimited by a network of fibrillar structural elements with a diameter in the range 20-50 nm, as evidenced by scanning electron microscopy.[13-15]

Pore size of materials with cavities smaller than 50 nm and surface area can be easily measured by nitrogen adsorption methods.[16, 17] In this work, such techniques, typically used for the characterization of adsorbents or inorganic catalysts, have been applied to the study of the texture of alginate aerogels. Supercritical CO_2 drying of alcogels has been suggested as the best method to obtain an image of the wet materials in the solid state. This procedure releases the porous texture quite intact by avoiding the pore collapse phenomenon.[9, 18]

. An investigation of the textural properties of alginate aerogels of three different compositions in term of mannuronic/guluronic ratio is reported. Scanning electron microscopy observations have been associated to the analysis of N_2 sorption isotherms.

Experimental

The characteristics of the three different sodium alginates used in this work are reported in table 1.

Table 1. Characteristics of the alginates samples.

Sample	Guluronic percent (by ^{13}C NMR)	viscosity 2 % solution (w/v) η(mPa.s^{-1})	average Mw
G-20	20	200	200 000
G-45	45	2000	400 000
G-76	76	2000	400 000

Sodium alginate was dissolved in distilled water at a concentration of 2% (w/v). The polymer solution was added dropwise at room temperature to the stirred $CaCl_2$ (Aldrich) solution (0.24 M) using a syringe with a 0.8mm diameter needle. The microspheres were cured in the gelation solution for a given time. The maturation time, 1 hour for G-20, 3 hours for G-45 and G-76, was chosen as the time providing the highest surface area at the end of the preparation. The microspheres were then dehydrated by immersion in a series of successive ethanol-water baths of increasing alcohol concentration (10, 30, 50, 70, 90, 100 %) during 15 min each.[18] Then, the microspheres were dried under supercritical CO_2 conditions (74 bars, 31.5°C) in a Polaron 3100 apparatus.

Scanning electron micrographs (SEM) of cross-sections of the dried microspheres were obtained on an Hitachi apparatus after platinum metallization.

Nitrogen adsorption/desorption isotherms were recorded in a Micromeritics ASAP 2010 apparatus at 77 K after outgassing the sample at 353 K under vacuum until a stable $3 \cdot 10^{-5}$ Torr pressure was obtained without pumping. A reference isotherm was measured on fumed silica Aerosil 200 and used for comparison plots in the relative pressure range 0.05-0.93.

Results and Discussion

The properties of alginate gels are influenced by the ratio and sequencing of the uronic monomers,[19] the concentration of the cation in the maturation bath and the time of maturation.[20, 21] Three different alginates were used for this study, with different guluronic fractions: G-20 (20 % guluronic), G-45 (45 % guluronic) and G-76 (76 % guluronic).

Gel spheres obtained from alginate G-45 are represented in Figure 2 at different stages of preparation: hydrogel spheres (Figure 2a), alcogel spheres obtained after exchange of water by ethanol (Figure 2b), and aerogel spheres obtained after supercritical CO_2 drying (Figure 2c). For sake of comparison, the xerogel spheres obtained from the alcogel by ethanol evaporation at room temperature are also represented (Figure 2d). For all alginate samples, the average sphere diameter at the different stages of preparation is reported in Table 2.

Table 2. Average bead size and mean square error (mm) for three different alginates at different stages of preparation.

	G-20	G-45	G-76
hydrogel	3.03 ± 0.11	2.72 ± 0.17	2.76 ± 0.13
alcogel	2.76 ± 0.13	2.53 ± 0.13	2.63 ± 0.19
aerogel	2.81 ± 0.24	2.50 ± 0.14	2.35 ± 0.11
xerogel	0.87 ± 0.08	0.83 ± 0.03	0.90 ± 0.04

For all alginate samples, the exchange of ethanol for water brought about a size shrinkage lower than 10 %, corresponding to a volume shrinkage lower than 25 %, in good agreement with literature results.[18, 22] The supercritical CO_2 drying allows to form the aerogel from the alcogel and brings about no size change of the spheres of G-20 and G-45. The shrinking observed in the case of G-76 is at the limit of the mean square error and probably witnesses the experimental problems that sometimes affect supercritical drying.[21]

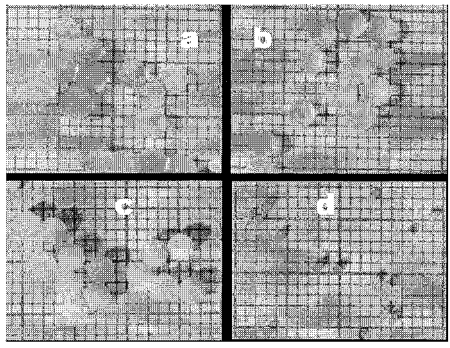

Figure 2. G-45 alginate beads at different phases of the preparation. (a) hydrogel, (b) alcogel, (c) aerogel from supercritical CO_2-dried alcogel, (d) xerogel from room temperature-dried alcogel. Grid square side 1 mm.

By contrast, the ethanol evaporation in room conditions forms a xerogel and brings about a dramatic shrinking of the alginate spheres. The size of the xerogel spheres is about 30 % of the size of the hydrogel spheres, hence the xerogel volume is 2.7 % of the volume of the hydrogel. This data has to be compared with the concentration of the initial alginate solution, 2 % (w/v), and indicates that the alcohol evaporation has produced a compact alginate with virtually no porous structure.

Scanning electron micrographs of cross-sections of the aerogels obtained from the three alginate samples are reported in Figure 3.

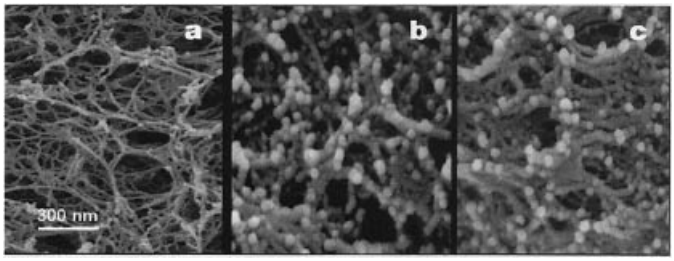

Figure 3. Scanning electron microscopy of cross-sections of alginate aerogels. (a) G-20, (b) G-45, and (c) G-76. Same scale for all pictures.

The texture of the G-20 aerogel is an open network of fibres with diameter 10-15 nm, in good agreement with previous reports.[10, 13, 15] The nanostructure of the G-45 and G-76 aerogels is instead characterized by important instances of aggregations and is constituted by strings of nanobeads with diameter 20-30 nm. Bead strings are frequently associated to form pillars and, in the case of G-76, sheets. The aerogels from guluronic-rich alginates present a more compact nanostructure than the mannuronic-rich sample, seemingly in agreement with the better mechanical properties of the guluronic-rich gels.[19]

Nitrogen adsorption-desorption isotherms provide useful information about several textural properties.[16, 17] The adsorption at low relative pressure allows to evaluate the surface area of the sample or the presence of microporosity. Microporosity can be differentiated from monolayer adsorption by drawing comparison plots, in which the volume adsorbed is plotted as a function of the volume adsorbed at the same pressure on a reference non-porous specimen. Several kinds of comparison plots are commonly used and the alpha-S plot, in which the unit value of the X axis corresponds to the volume adsorbed at relative pressure 0.40 on the reference isotherm, has been used in this communication. The presence of micropores is expected to be indicated by a positive extrapolated value of the comparison plot at alpha-S = 0.

Linear portions of the comparison plot correspond to pressure domains in which the adsorption takes place with the same mechanism as on the reference adsorbent, expectedly a monolayer-multilayer mechanism. Positive deviations from linearity corresponds to condensation phenomena and allows to quantitatively evaluate the presence of mesopores.

The surface area can be evaluated by the classical BET method or by the slope of the alpha-S plot. This last method is expected not to be affected by the presence of micropores.

The adsorption-desorption isotherms of N_2 at 77 K on the three alginate aerogels are presented in Figure 4 and the corresponding alpha-S plots are presented in Figure 5.

All isotherms of Figure 4 are type IV, typical of mesoporous solids with strong adsorbent-adsorbate interaction. The well-defined step at low relative pressure corresponds to a high energy of monolayer adsorption. This effect is confirmed by the high C_{BET} parameter, about 140, reported in Table 3. Such a strong low-pressure adsorption can easily hid the presence of micropores, and indeed the comparison plots extrapolated at alpha-S = 0 indicate the presence of some microporosity in all samples (Figure5).

The micropore volume, reported in table 3, is very small, the observed value of 0.014 cm^3 g^{-1} corresponding to the adsorption of a nitrogen molecule per 12 uronic units, and indicates that the alginate at 77 K is quite impervious to the N_2 molecules. If it is taken into account that the reference used in the comparison plot, a fumed silica, has not the same composition as the polysaccharide samples, the measured micropore volume could also be attributed to a different shape of the adsorption isotherm on the highly polar surface of the alginate.

Table 3. Textural data from N_2 adsorption isotherms at 77 K.

	S-20	S-45	S-76
BET surface area (m^2 g^{-1})	342	339	507
alpha-S surface area (m^2 g^{-1})	314	302	470
micropore volume (cm^3 g^{-1})	0.009	0.014	0.013
C_{BET}	138	144	142
calculated fibre diameter (nm)	12.7	13.3	8.5
calculated nanobead diameter (nm)	19.0	20.0	12.8

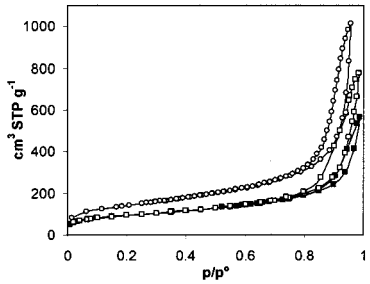

Figure 4. N_2 adsorption-desorption isotherms at 77 K for three alginate aerogels: (filled squares) G-20, (empty squares) G-45, (empty circles) G-76.

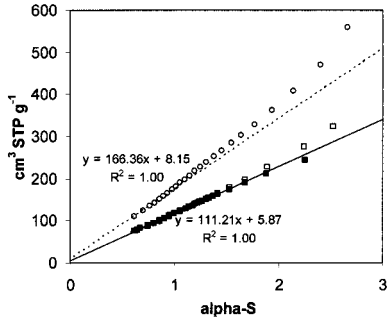

Figure 5. Alpha-S plots for three alginate aerogels: (filled squares) G-20, (empty squares) G-45, (empty circles) G-76. The linear parts of the plots for G-20 (full line) and G-76 (dotted line) are evidenced. The linear part of the G-45 curve, very similar to G-20, is omitted for sake of clarity.

The slow steady rise beyond p/p° 0.1 of the isotherms of Figure 4 indicates the absence of any small mesoporosity. No hysteresis can be observed below relative pressure 0.8 which, in the case of cylindrical pores, would correspond to a smallest mesopore size limit of 13 nm.[23] At higher pressure, the mesopore distribution is open, with no solution of continuity with the macroporous domain.

In very open networks, as those presented by the samples under examination, only a limited fraction of the surface corresponds to the inner surface of mesopores and a reliable evaluation of the mesopore volume has not to take into account most of the adsorbate related to a monolayer-multilayer adsorption mechanism. In this case, the amount of condensate by capillarity can be easily measured on the comparison plots (Fig. 5) as the difference between the adsorbed volume and the extrapolation at high pressure of the

linear portion of the alpha-S plot. In the case of the sample with the largest mesoporosity, the gel G-76, the volume adsorbed in mesopores with diameter smaller than 25 nm does not exceed 0.15 $cm^3 g^{-1}$.

In the case of gels G-20, the alpha-S plot reported in Figure 5 presents a slight but significant negative deviation at high relative pressure. This indicates that the sample presents less mesoporosity than the reference sample which, contrarily to expectations, presents some intergranular porosity and traces of hysteresis beyond p/p° 0.8.

The observed mesoporosity can be related to the gel morphology observed by electron microscopy. The gel G-20, virtually not mesoporous, is formed by an open network of isolated fibres. The gels G-45 and G-76, with significant mesoporosity, are formed by aggregated strings of nanobeads. It seems clear that the mesoporosity has to be attributed to cavities among aggregated strings, inside the strands which provide the mechanical stiffness of the guluronic-rich gels.

The BET surface area of the samples, reported in Table 3, is likely affected by the presence of microporosity. In this case, the slightly lower value calculated by the slope of the alpha-S plot is a more reliable evaluation of the surface area. This evaluation of the surface area, in the hypothesis of homogeneity of each sample, can provide some information on the size of the structural elements. It is easy to calculate the diameter of cylinders or spheres which would present the measured surface area, under the assumption of a density value for the material (unit density in this calculation). The calculated diameters are reported in Table 3. In the case of the sample G-20, a spherical model largely overestimates the size of the fibres, while a cylindrical model indicates a diameter 13 nm for the fibres, in good agreeement with electron microscopy results. In the case of the samples G-45 and G-76, a cylindrical model grossly underevaluates the size of the structural elements, while a spherical model approaches the size of the nanobeads observed by electron microscopy.

Conclusions

Nitrogen adsorption provides useful information for the characterisation of polysaccharide aerogels. Adsorption techniques alone provide quantitative data on surface area and microporous and mesoporous volume. The obtention of textural information from these data is only possible if independent information, provided by scanning electron microscopy, allows to choose between several possible models. The structure of alginate aerogels of different composition has been successfully determined by the use of these

complementary techniques. The results suggest that CO_2 supercritical drying does not alter the texture of the original gel.

[1] G. T. Grant, E. R. Morris, D.A. Rees, P. J. Smith, D. Thom, *FEBS Lett.* **1973**, *32*, 195.
[2] M. Grassi, I. Colombo, R. Lapasin, *J. Control. Release* **2001**, *76*, 93.
[3] M. Kierstan, C. Bucke, *Biotechnol. Bioeng.* **2000**, *76*, 726.
[4] C. Stabler, K. Wilks, A. Sambanis, I. Constantinidis, *Biomaterials* **2001**, *22*, 1301.
[5] A. Blandini, M. Macias, D. Cantero, *Enzyme Microb. Technol.* **2000**, *27*, 319.
[6] S.C. Musgrave, N.W. Kerby, G.A. Codd, W.D.P. Stewart, *Eur. J. Appl. Microbiol. Biotechnol.* **1983**, *17*, 133.
[7] P. Scherer, M. Kluge, J. Klein, H. Sahm, *Biotechnol. Bioeng.* **1983**, *23*, 1057.
[8] D. Casson, A.N. Emery, *Enzyme Microb. Technol.* **1987**, *9*, 102.
[9] B.P. Hills, J. Godward, M. Debatty, L. Barras, C.P. Saturio, C. Ouwerx, *Magn. Res. Chem.* **2000**, *38*, 719.
[10] D. Serp, M. Mueller, U. Von Stocker, I.W. Marison, *Biotech. Bioeng.* **2002**, *79*, 253.
[11] H. Tanaka, M. Matsurama, I. Veliky, *Biotech. Bioeng.* **1994**, *26*, 53.
[12] M. Longo, I. Novella, L. Garcia, M. Diaz, *Enzyme Microb. Technol.* **1991**, *14*, *586*.
[13] Y.M. Belatseva, V.B. Tolstognzov, D.B. Izymov, M.M. Genia, *Biofizika* **1972**, *17*, 744.
[14] F. Yokoyama, C. Achife, K. Takakira, Y. Yamashita, K. Monebe, *J. Macromol. Sci. Phys.* **1992**, *B31*, 463.
[15] D. Serp, M. Mueller, U. Von Stocker, I.W. Marison, *Biotech. Bioeng.* **2002**, *79*, 243.
[16] S. J. Gregg and K. S. W. Sing., "*Adsorption, Surface Area and Porosity*", Academic Press, London 1982.
[17] F. Rouquerol, J. Rouquerol, K. Sing, "*Adsorption by powders and porous solids*", Academic Press, San Diego 1999.
[18] A. Martinsen, I. Storrø, G. Skjåk-Bræk, *Biotech. Bioeng.* **1992**, *39*, 186.
[19] O. Smidsrød, *Faraday Discuss. Chem. Soc.* **1974**, *57*, 263.
[20] N. Velings, M.M. Mestdagh, *Polym. Gels Netw.* **1995**, *3*, 311.
[21] C. Ouverx, N. Velings, M.M. Mestdagh, M.A.V. Axelos, *Polym. Gels Netw.* **1998**, *6*, 393.
[22] B. Thu, O. Gåserød, D. Paus, A. Mikkelsen, G. Skjåk-Bræk, R. Toffanin, F. Vittur, R. Rizzo, *Biopolymers* **2000**, *53*, 60.
[23] J.C.P. Broekhoff, J.H. de Boer, *J. Catal.* **1968**, *10*, 377.